Japanese Journal of Applied Physics **58**, 010909 (2019) **RAPID COMMUNICATION**
https://doi.org/10.7567/1347-4065/aaf3aa

286 nm monolithic multicomponent system

Jialei Yuan[1], Yan Jiang[1], Zheng Shi[1], Xumin Gao[1], Yongjin Wang[1,2*], Xiaojuan Sun[3], Dabing Li[3*], Yuhuai Liu[4*], and Hiroshi Amano[5*]

[1]*Peter Grünberg Research Centre, Nanjing University of Posts and Telecommunications, Nanjing 210003, People's Republic of China*
[2]*Key Laboratory of Broadband Wireless Communication and Sensor Network Technology (Nanjing University of Posts and Telecommunications), Ministry of Education, Nanjing 210003, People's Republic of China*
[3]*State Key Laboratory of Luminescence and Applications, Changchun Institute of Optics, Fine Mechanics and Physics, Chinese Academy of Sciences, Changchun 130033, People's Republic of China*
[4]*Department of Electronics Engineering, Zhengzhou University, Science Road 100, Zhengzhou 450001, People's Republic of China*
[5]*Institute of Materials and Systems for Sustainability, Nagoya University, Nagoya 464-8062, Japan*

*E-mail: wangyj@njupt.edu.cn; lidb@ciomp.ac.cn; ieyhliu@zzu.edu.cn; amano@nuee.nagoya-u.ac.jp

Received October 15, 2018; accepted November 22, 2018; published online December 12, 2018

We present a 286 nm monolithic multicomponent system in which two identical multiple quantum well (MQW) diodes merge with a waveguide together on a single chip. The monolithic multicomponent system allows all existing standard fabrication processes and establishes an optical link between two MQW-diodes because of the simultaneous emission-detection phenomenon. One MQW-diode transcribes electronic information into an optical signal to be coupled into a waveguide. The guided light then propagates along the waveguide to the other MQW-diode that converts the optical signal into an electronic one. A spatial light transmission at 50 Mbps is demonstrated using non-return-to-zero on–off keying modulation.

With increasing demands for purification, sensing, surface sterilization, biochemistry and on-chip electronic–photonic system,[1–8)] AlGaN-based multiple quantum well diode (MQW-diode) is attractive for the development of multicomponent system on a chip. MQW-diode can function as a light-emitting diode to generate light or a photodiode to detect light.[9–11)] In particular, the simultaneous emission-detection phenomenon (SEDP) occurs when the applied voltage to the MQW-diode is higher than threshold voltage and the high-energy incoming light shines on the MQW-diode,[12,13)] whereby the device can transmit and receive information through light at the same time. Information superimposition that is the adding together of input and output signals can be decoded using a self-interference cancellation method. Advanced information system will then be brought into reality as novel signal processing methods are employed. Multifunctioning optoelectronic devices are of great interest for the fabrication of monolithic multicomponent system towards the Internet of Things.[14–16)] Up to date, a variety of multicomponent systems on a chip have been manufactured on different material platforms.[17–25)] Furthermore, it should be noted that III-nitride platform for photonics can accommodate the electronics, which allows all existing standard fabrication processes to produce monolithic electronic–photonic circuit without any extra investments.

Here, we propose the fabrication and characterization of a monolithic III-nitride electronic–photonic system on a III-nitride-on-sapphire platform. Merging two identical 286 nm MQW-diodes together on a single chip is developed for diverse applications in the deep-ultraviolet (DUV) range. Sharing identical MQWs structure, two MQW-diodes are produced by using the same fabrication process flow and separately function as a transmitter and receiver. Two independent components can communicate with each other using light guided by a waveguide, leading to a multicomponent system with enhanced functionalities.

On the basis of the SEDP, the MQW-diode not only emits light, but also absorbs short-wavelength light generated by itself because the dual-functioning devices intrinsically has a spectral overlap between the EL spectra and the detection spectra. Figure 1 schematically illustrates the operation mechanisms of monolithic III-nitride multicomponent system. When two identical MQW-diodes are produced on a chip and interconnected with a waveguide, high-energy light generated by one MQW-diode will propagate along the waveguide and shine on the junction of another MQW-diode to produce the photogenerated current. The resulting integrated system on a chip enables data transmission using optical link between two MQW-diodes. One MQW-diode functions as a transmitter to deliver signals using modulated light. The coded light is coupled into the waveguide and guided to another MQW-diode, which serves as a receiver to convert the optical signals into electrical ones. Only a small fraction of the emitted light can directly irradiate another MQW-diode through free-space because two devices are fabricated on the same plane.[26)] Moreover, GaN-based integrated system is promising for the micro-total-analysis system for medical diagnosis and environmental analysis. The waveguide in our proposed monolithic multicomponent system will be further optimized for isolation trench and liquid or gas flow channel.[27)] When exposed to DUV light, a photochemical process occurs to reduce contaminants in air or water. The DUV monolithic multicomponent system will thus pave the way towards the development of sensor for bacterial density in a water or air, air pollution sensor, etc.

Figure 2(a) shows a cross-sectional scanning electron microscope (SEM) image of III-nitride on a sapphire substrate. A 2500 nm thick AlN buffer layer is deposited on sapphire substrate. A 600 nm thick undoped AlGaN layer is subsequently grown, followed by 1750 nm thick n-type AlGaN layer. MQW structure has a thickness of 130 nm. After growing p-type electron blocking layer, a p-type GaN layer is finally deposited. The total thickness is around 5230 nm. The monolithic multicomponent system is produced by the utilization of existing fabrication processes. Isolation mesas are defined by photolithography, and inductively coupled plasma reactive ion etching is employed to expose the n-type AlGaN using Cl_2 and BCl_3 hybrid gases with flow rates of 10 and 25 sccm, respectively. Following

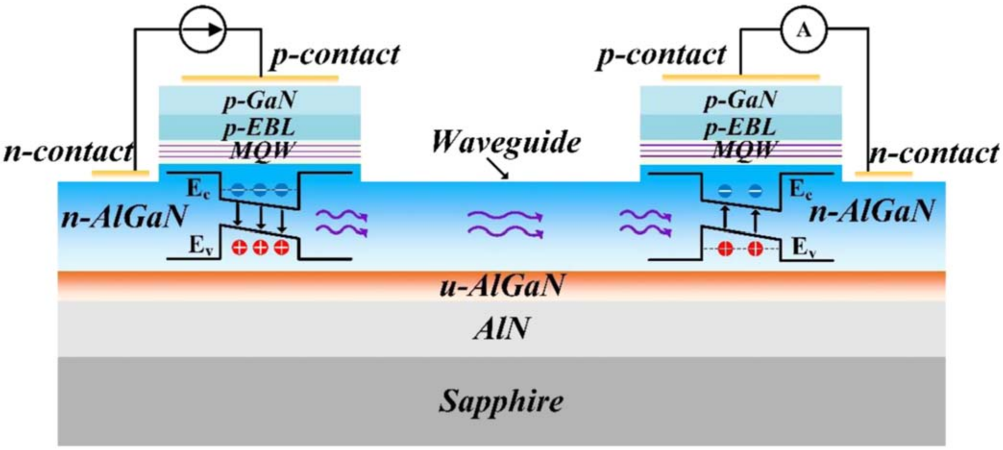

Fig. 1. (Color online) Schematic operation mechanisms of monolithic III-nitride multicomponent system.

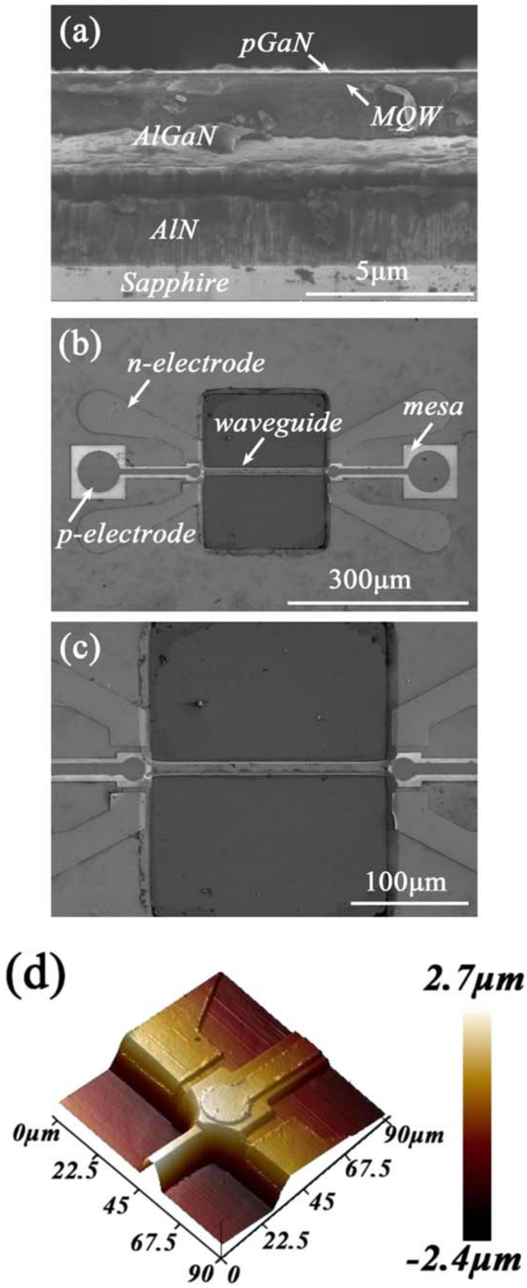

Fig. 2. (Color online) (a) Cross-sectional SEM image of III-nitride films on sapphire substrate. (b) SEM image of the monolithic multicomponent system on sapphire. (c) Magnified SEM image of the coupling butts consisting of the MQW-diode and waveguide. (d) Three-dimensional AFM image of the coupling butts.

electron beam evaporation and lift-off processes, both p- and n-contacts are obtained with 30/400 nm Ni/Ag metal stacks, leading to the formation of the MQW-diodes. Waveguides are then defined and etched down to sapphire substrate. After removing residual photoresist by O_2 ashing, optical interconnect between two MQW-diodes using a waveguide is generated to realize the multicomponent system on a chip.

Figure 2(b) shows a SEM image of the monolithic III-nitride multicomponent system on sapphire in which two identical MQW-diodes merge a waveguide together. One MQW-diode functions as a transmitter to emit the modulated light to be coupled into the 10 μm wide and 100 μm long waveguide. The guided light propagates along the waveguide and is directed to the other MQW-diode that serves as a photodiode to convert the optical information into the electronic signals. Two MQW-diodes communicate with each other using 286 nm light, establishing on-chip light communication in the multicomponent system. Figure 2(c) shows a magnified SEM image of the coupling butts. The p-type GaN and MQW layers on the waveguide are etched away to obtain device isolation between two MQW-diodes, which will negatively affect the coupling efficiency between the MQW-diode and waveguide. Figure 2(d) shows a three-dimensional atomic force microscope (AFM) image of the coupling butts. The generated mesa is approximately 700 nm in height and the gap between the n-electrode and mesa is about 5 μm. Because the index contrast between III-nitride and sapphire is small, the downward light propagation readily leads to optical leakage into the transparent sapphire and optical crosstalk between other channels. Selective-area sapphire removal to obtain suspended device architecture will be a feasible route to eliminate these challenging issues.[28]

Figure 3(a) shows the measured current–voltage (I–V) curve of the MQW-diode on sapphire. The rectifying behavior is clearly observed for the MQW-diode. The inset is the light emission image when two MQW-diodes are simultaneously biased at 12 V using an AVTECH pulse generator. The frequency and the pulse width are 1.0 MHz and 50 ns, respectively. A fiber probe directly collects the emitted light to send to an Ocean Optics HR4000 spectrometer for characterization. Figure 3(b) summarizes the electroluminescence (EL) spectra as a function of the forward voltage of the MQW-diode. The electron-to-photon conversion is proportional to the forward voltage. In response to changes in the forward voltage from 11 to 17 V, the emission intensity is significantly increased. A dominant EL peak is observed at 286.4 nm with a full width at half maximum of 9.6 nm at the forward voltage of 17 V. It should be noted that the peak wavelength of the MQW-diode almost remains stable. The emitted light is self-absorbed to excite light at longer wavelengths, leading to a limitation in the emission efficiency. The guided light propagates along the waveguide and is directed to another MQW-diode, which generates a proportional photocurrent. An on-chip optical interconnection is thus established by the multicomponent system,[29–32] in which one MQW-diode is used as the transmitter to convert the electronic signals into optical ones, and another MQW-diode serves as the receiver to complete photon-to-electron conversion. The transmitter converts electronic signals into a proportional modulated light. With increasing the injection current of the transmitter, much more photons are generated and transmitted to the receiver. As a result, the induced photocurrent at the receiver is increased. Dynamically on-chip monitoring the changes in the injection current is possible. Figure 3(c) shows the dependence of the induced photocurrent at the receiver on the injection current of the transmitter. When the receiver is zero-biased, the photocurrent is increased from 7.3 to 20.6 nA as the injection current of the transmitter is increased from 10 to 40 μA. In the on-chip optical link, the transmitter at one end to code the information at one end, the modulated light that travels along the waveguide is directed to the receiver at the other end. A Keysight 33 600 A arbitrary waveform generator directly modulate the transmitter with the peak-to-peak voltages V_{pp} of 5.0 V and the offset voltages V_{offset} of 5.0 V to code the information into the optical signals. The modulation frequency is 1.0 MHz with the filling factor of 0.5. At the other end, the receiver converts the optical signals into electrical ones to be directly sent to a digital storage oscilloscope for characterization. Figure 3(d) shows the received signals in the on-chip optical link when the receiver operates under a photodetection mode with zero-bias voltage applied. The receiver converts optical information into electrical signals, which are consistent with the original electrical ones. Optical interconnections with capability of on-chip data communication is possible using the proposed GaN-based photonic multicomponent.

To demonstrate spatial communication using DUV light, a large MQW-diode with ring geometry that is fabricated on the same substrate is used because the light emission is limited by the device size. Figure 4(a) shows an optical microscope image of a ring MQW-diode. The 170 μm wide ring p-electrode has a 1.23 mm diameter inner region to balance emission and conduction performance. The large area MQW-diode can increase the emission intensity, but at the same time, it increases the capacitance component, which may provide a negative consequence on the device performance particularly in terms of signal communication. Decreasing the device size will be an effective way to increase the response rate if the emission intensity is high enough to be detected.[33,34] Using non-return-to-zero on–off keying modulation, the wire-bonded MQW-diode is modulated by an arbitrary waveform generator, whereby the 1.0 V V_{pp} of and 9.5 V V_{offset} are applied. The light is coded with the pseudorandom binary sequence (2^7-1) data streams and sensed by a Hamamatsu C12702-11

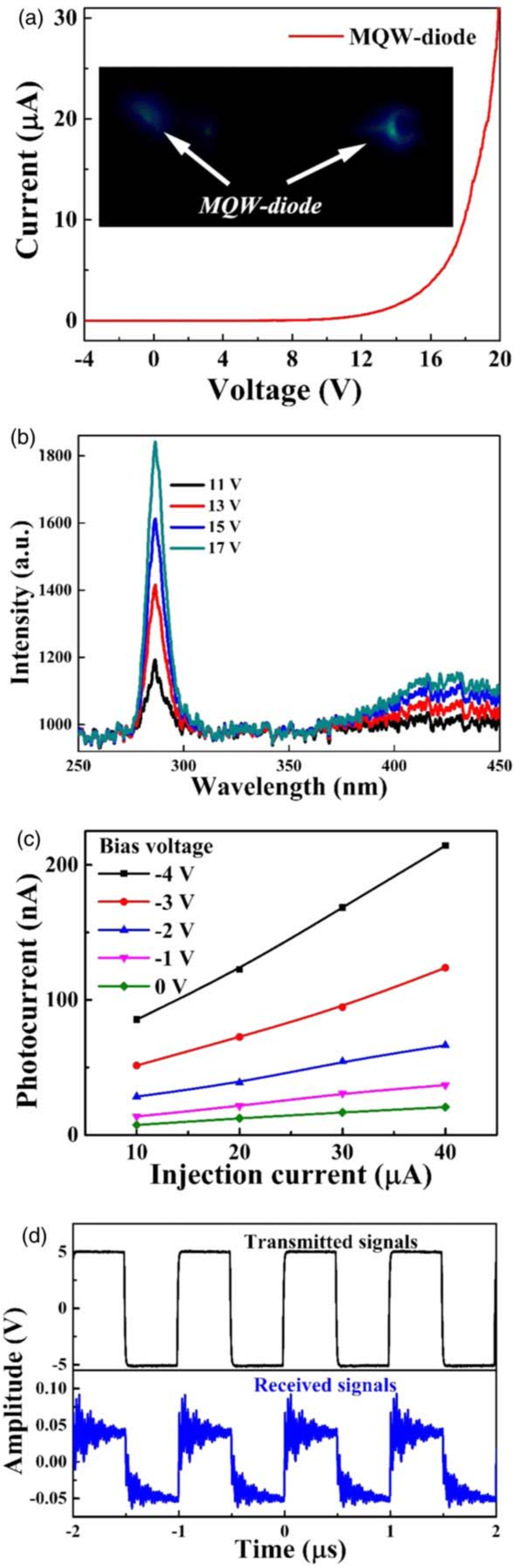

Fig. 3. (Color online) (a) Measured *I–V* curve of the MQW-diode, and the inset is the light emission image. (b) EL spectra of the MQW-diode. (c) Induced photocurrent at the receiver vs. the injection current of the transmitter. (d) Square-wave signals received at different bias voltages.

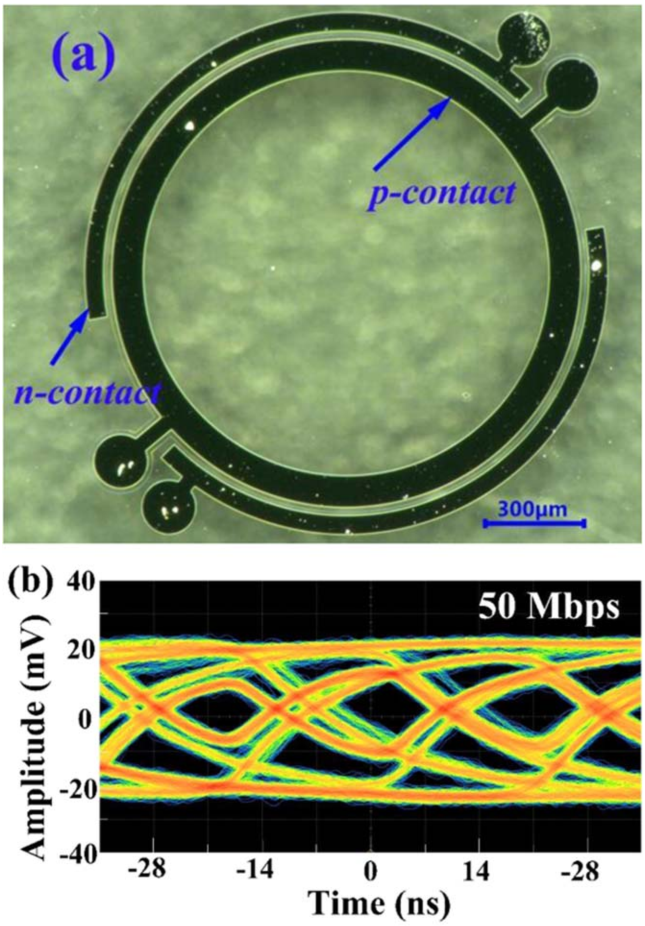

Fig. 4. (Color online) (a) Optical microscope image of the MQW-diode with ring geometry. (b) Eye diagrams for free-space light communication at a transmission rate of 50 Mbps.

photodiode module through a micro-transmittance setup. The optical signals are converted into electrical ones, which are sent to a digital storage oscilloscope for characterization. The oscilloscope operates under AC coupling model with an input impedance of 1 MΩ. Figure 4(b) shows error-free eyes at a rate of 50 Mbps. According to the eye diagrams, the signal-to-noise ratio is calculated to be 7.04 dB, and the bit error rate is approximately 7.36×10^{-4}.

A 286 nm monolithic multicomponent system is implemented on a III-nitride-on-sapphire platform by the utilization of all existing fabrication processes. According to SEDP, on-chip optical link using a waveguide is built up between two identical MQW-diodes, which separately function as a transmitter and receiver. The multicomponent system enables light communication on the chips, paving the way for the development of advanced information system towards the Internet of Things in the DUV region.

Acknowledgments This work was jointly supported by the Natural Science Foundation of Jiangsu Province (BE2016186), National Natural Science Foundation of China (61531166004), National Key R&D Program of China (2016YFE0118400), "111" project, National Science Fund for Distinguished Young Scholars (61725403) and CAS Interdisciplinary Innovation Team.

1) H. Hirayama, N. Maeda, S. Fujikawa, S. Toyoda, and N. Kamata, "Recent progress and future prospects of AlGaN-based high-efficiency deep-ultraviolet light-emitting diodes," Jpn. J. Appl. Phys. **53**, 100209 (2014).
2) H. Hirayama, S. Fujikawa, N. Noguchi, J. Norimatsu, T. Takano, K. Tsubaki, and N. Kamata, "222–282 nm AlGaN and InAlGaN-based deep-UV LEDs fabricated on high-quality AlN on sapphire," Phys. Status Solidi A **206**, 1176 (2009).
3) T. Kinoshita et al., "Deep-ultraviolet light-emitting diodes fabricated on AlN substrates prepared by hydride vapor phase epitaxy," Appl. Phys. Express **6**, 092103 (2013).
4) Y. Aoyagi, M. Takeuchi, K. Yoshida, M. Kurouchi, T. Araki, Y. Nanishi, H. Sugano, Y. Ahiko, and H. Nakamura, "High-sensitivity ozone sensing using 280 nm deep ultraviolet light-emitting diode for detection of natural hazard ozone," J. Environ. Prot. **3**, 695 (2012).
5) R. Jain et al., "Migration enhanced lateral epitaxial overgrowth of AlN and AlGaN for high reliability deep ultraviolet light emitting diodes," Appl. Phys. Lett. **93**, 5532 (2008).
6) M. S. Shur and R. Gaska, "Deep-ultraviolet light-emitting diodes," IEEE Trans. Electron Devices **57**, 12 (2009).
7) M. Shatalov et al., "High power AlGaN ultraviolet light emitters," Semicond. Sci. Technol. **29**, 1779 (2014).
8) H. M. Chang, W. C. Lai, W. S. Chen, and S. J. Chang, "GaN-based ultraviolet light-emitting diodes with AlN/GaN/InGaN multiple quantum wells," Opt. Express **23**, A337 (2015).
9) Y. Nanishi, "Nobel prize in physics: the birth of the blue LED," Nat. Photonics **8**, 884 (2014).
10) G. Q. Li, W. L. Wang, W. J. Yang, Y. H. Lin, H. Y. Wang, Z. T. Lin, and S. Z. Zhou, "GaN-based light-emitting diodes on various substrates: a critical review," Rep. Prog. Phys. **79**, 056501 (2016).
11) D. B. Li, K. Jiang, X. J. Sun, and C. L. Guo, "AlGaN photonics: recent advances in materials and ultraviolet devices," Adv. Opt. Photonics **10**, 43 (2018).
12) Y. J. Wang, Y. Xu, Y. C. Yang, X. M. Gao, B. C. Zhu, W. Cai, J. L. Yuan, R. Zhang, and H. B. Zhu, "Simultaneous light emission and detection of InGaN/GaN multiple quantum well diodes for in-plane visible light communication on a chip," Opt. Commun. **387**, 440 (2017).
13) Y. J. Wang, X. Wang, B. C. Zhu, Z. Shi, J. L. Yuan, X. M. Gao, Y. H. Liu, X. J. Sun, D. B. Li, and H. Amano, "Full-duplex light communication with a monolithic multicomponent system," Light: Sci. Appl. **7**, 83 (2018).
14) N. Oh et al., "Double-heterojunction nanorod light-responsive LEDs for display applications," Science **355**, 616 (2017).
15) Y. R. Jiang, S. Y. Yong Cho, and M. Shim, "Light-emitting diodes of colloidal quantum dots and nanorod heterostructures for future emissive displays," J. Mater. Chem. C **6**, 2618 (2018).
16) H. Zhang and J. A. Rogers, "Recent advances in flexible inorganic light emitting diodes: from materials design to integrated optoelectronic platforms," Adv. Opt. Mater. **2018**, 1800936 (2018).
17) Z. Y. Jiang, M. R. M. Atalla, G. J. You, L. Wang, X. Y. Li, J. Liu, A. M. Elahi, L. Wei, and J. Xu, "Monolithic integration of nitride light emitting diodes and photodetectors for bi-directional optical communication," Opt. Lett. **39**, 5657 (2014).
18) Y. J. Lee, Z. P. Yang, P. G. Chen, Y. A. Hsieh, Y. C. Yao, M. H. Liao, M. H. Lee, M. T. Wang, and J. M. Hwang, "Monolithic integration of GaN-based light-emitting diodes and metal-oxide-semiconductor field-effect transistors," Opt. Express **22**, A1589 (2014).
19) C. Liu, Y. F. Cai, Z. J. Liu, J. Ma, and K. M. Lau, "Metal-interconnection-free integration of InGaN/GaN light emitting diodes with AlGaN/GaN high electron mobility transistors," Appl. Phys. Lett. **106**, 181110 (2015).
20) K. Tsuchiyama, K. Yamane, S. Utsunomiya, H. Sekiguchi, H. Okada, and A. Wakahara, "Monolithic integration of Si-MOSFET and GaN-LED using Si/SiO_2/GaN-LED wafer," Appl. Phys. Express **9**, 104101 (2016).
21) W. Cai, Y. C. Yang, X. M. Gao, J. L. Yuan, W. Yuan, H. B. Zhu, and Y. J. Wang, "On-chip integration of suspended InGaN/GaN multiple-quantum-well devices with versatile functionalities," Opt. Express **24**, 6004 (2016).
22) C. Shen et al., "High-modulation-efficiency, integrated waveguide modulator-laser diode at 448 nm," ACS Photonics **3**, 262 (2016).
23) M. X. Feng et al., "On-chip integration of GaN-based laser, modulator, and photodetector grown on Si," IEEE J. Sel. Top. Quantum Electron. **24**, 8200305 (2018).
24) K. H. Li, W. Y. Fu, Y. F. Cheung, K. K. Y. Wong, Y. Wang, K. M. Lau, and H. W. Choi, "Monolithically integrated InGaN/GaN light-emitting diodes, photodetectors, and waveguides on Si substrate," Optica **5**, 564 (2018).
25) C. Liu, Y. F. Cai, H. X. Jiang, and K. M. Lau, "Monolithic integration of III-nitride voltage-controlled light emitters with dual-wavelength photodiodes by selective-area epitaxy," Opt. Lett. **43**, 3401 (2018).
26) X. M. Gao, J. L. Yuan, Y. C. Yang, Y. H. Li, W. Cai, X. Li, and Y. J. Wang, "Light coupling for on-chip optical interconnects," Opt. Laser Technol. **97**, 154 (2017).

27) K. H. Li, Y. F. Cheung, W. Y. Fu, K. K. Y. Wong, and H. W. Choi, "Monolithic integration of GaN-on-sapphire light-emitting diodes, photodetectors, and waveguides," IEEE J. Sel. Top. Quantum Electron. **24**, 3801706 (2018).
28) H. Nakazato, H. Kawaguchi, A. Iwabuchib, and K. Hane, "Micro fluorescent analysis system integrating GaN-light-emitting-diode on a silicon platform," Lab Chip **12**, 3419 (2012).
29) A. H. Atabaki et al., "Integrating photonics with silicon nanoelectronics for the next generation of systems on a chip," Nature **556**, 349 (2018).
30) C. Sun et al., "Single-chip microprocessor that communicate directly using light," Nature **528**, 534 (2015).
31) L. Vivien, "Silicon chips lighten up," Nature **528**, 483 (2015).
32) Y. J. Wang, X. Wang, J. L. Yuan, X. M. Gao, and B. C. Zhu, "Monolithic III-nitride photonic circuit towards on-chip optical interconnection," Appl. Phys. Express **11**, 122201 (2018).
33) W. Yang et al., "Size-dependent capacitance study on InGaN-based micro-light-emitting diodes," J. Appl. Phys. **116**, 044512 (2014).
34) R. Koester, D. Sager, W. A. Quitsch, O. Pfingsten, A. Poloczek, S. Blumenthal, G. Keller, W. Prost, G. Bacher, and F. J. Tegude, "High-speed GaN/GaInN nanowire array light-emitting diode on Silicon(111)," Nano Lett. **15**, 2318 (2015).